30. Fan, J., Griffiths, A. D., Lockhart, A., Cross, R. A. & Amos, L. A. Microtubule minus ends can be labeled with a phage display antibody specific to α-tubulin. *J. Mol. Biol.* **259,** 325–330 (1996).

Acknowledgements. We thank R. F. Ludueña for isotypically purified αβII and αβIII tubulin, M. Le for help with electron diffraction processing, and R. M. Glaeser and Y. L. Han for comments on the manuscript. Taxol was provided by the Drug Synthesis and Chemistry Branch, Division of Cancer Treatment of the National Cancer Institute. This work was supported by the NIH.

Correspondence and requests for materials should be addressed to E.N. Coordinates referred to in this Letter have been deposited in the Brookhaven Protein Data Bank with ID 1tub and will be accessible within one year.

Crystal structure of the bacterial cell-division protein FtsZ

Jan Löwe & Linda A. Amos

MRC Laboratory of Molecular Biology, Cambridge CB2 2QH, UK

Bacterial cell division ends with septation, the constriction of the cell wall and cell membranes that leads to the formation of two daughter cells[1,2]. During septation, FtsZ, a protein of relative molecular mass 40,000 which is ubiquitous in eubacteria and is also found in archaea and chloroplasts[3], localizes early at the division site to form a ring-shaped septum. This septum is required for the mechanochemical process of membrane constriction[4]. FtsZ is a GTPase[5,6] with weak sequence homology to tubulins[7]. The nature of FtsZ polymers *in vivo* is unknown, but FtsZ can form tubules, sheets and minirings *in vitro*[8,9]. Here we report the crystal structure at 2.8 Å resolution of recombinant FtsZ from the hyperthermophilic methanogen *Methanococcus jannaschii*. FtsZ has two domains, one of which is a GTPase domain with a fold related to one found in the proteins p21^{ras} and elongation factor EF-Tu. The carboxy-terminal domain, whose function is unknown, is a four-stranded β-sheet tilted by 90° against the β-sheet of the GTPase domain. The two domains are arranged around a central helix. GDP binding is different from that typically found in GTPases and involves four phosphate-binding loops and a sugar-binding loop in the first domain, with guanine being recognized by residues in the central connecting helix. The three-dimensional structure of FtsZ is similar to the structure of α- and β-tubulin[10].

Two FtsZ genes (named after filamenting temperature-sensitive mutant Z) from the archaeon *M. jannaschii* have been characterized by the genome project[11]. One gene, MJ0370, was amplified by genomic polymerase chain reaction (PCR) and expressed in *E. coli*/C41, a mutant of BL21 capable of expressing toxic genes[12]. Proteolysis during cell disruption was minimized by using heat-shock treatment. Cubic crystals were obtained and the structure was solved by multiple isomorphous replacement and density modification (see Methods and Table 1). The model (Fig. 1) contains residues 23–356, 116 water molecules, and one molecule of GDP; weak density for residues 1–22 was visible as an extension from helix H0.

FtsZ consists of two domains with a long, 23-residue, helix H5 (Figs 1a, 2) connecting them. The N-terminal portion of the molecule, containing residues 38–227, has GDP obtained from the expression host bound to it and will be called the GTPase domain. It consists of a six-stranded parallel β-sheet surrounded by two and three helices on both sides. The overall fold of the GTPase domain of FtsZ is related to typical GTPases and can be superimposed on the p21^{ras}–GDP complex (Protein Data Bank (PDB) entry 1Q21; ref. 13) using 52 Cα atoms (S1, H1, S2, H2, S4, H3 and S5) to give a root-mean-squared (r.m.s.) deviation of 1.88 Å. The topology of the β-sheet in FtsZ is 321456, which is slightly different from the topology in p21^{ras} (ref. 13), where it is 231456, but, together with the arrangement of five helices (H1, HL1, H2, H3 and H4), is consistent with typical Rossmann-fold topology[14]. Helix H2A is unique to FtsZ. Numbering of secondary structure elements (Fig. 2) follows the corresponding elements of p21^{ras} proteins.

The C-terminal domain, spanning residues 228–356, consists of a mainly parallel four-stranded central β-sheet supported by two helices on one side. The topology of the sheet is 1423, with strand 4 antiparallel to the others. The uncovered side of the sheet makes contacts with helix H5 and is otherwise open to the solvent. The fold of the C-terminal domain is related to chorismate mutase of *Bacillus subtilis* and can be superimposed on PDB entry 1COM[15] with an r.m.s. deviation of 1.83 Å over 52 Cα atoms (SC1, HC2, SC2, HC3, SC3 and SC4). Additionally, sequence comparisons give similarities to calmodulins in three loop regions (Swissprot CALM-TRYCR; loops between H5/HC1, SC1/HC2, and SC2/HC3) and to adenylyl cyclase (CYA1_HUMAN; residues 620–740), making a role in calcium binding feasible. The electrostatic potential on the

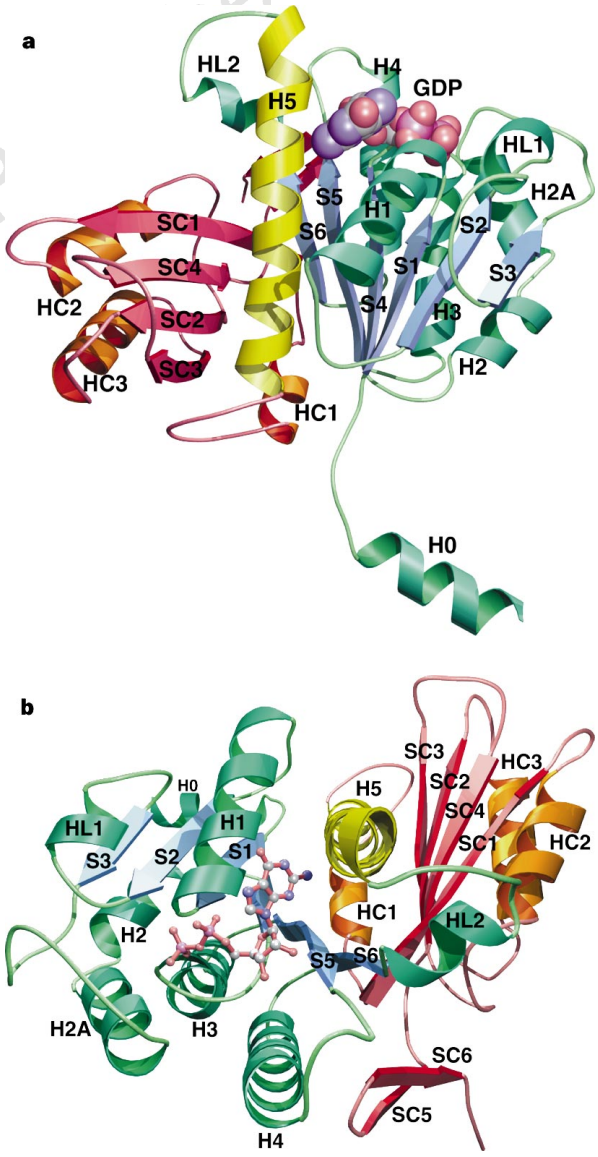

Figure 1 Ribbon drawings of FtsZ (residues 23–356) from *M. jannaschii*. **a**, View showing the GTPase domain in blue/green, the C-terminal domain in red/orange, and the connecting helix H5 in yellow. GDP is represented by a space-filling model. **b**, View of FtsZ rotated by ~90° from that in **a**. GDP is represented by a ball-and-stick model. Figures were prepared with POVSCRIPT (D. Peisach, personal communication)[28].

surface of the C-terminal domain is dominated by a large patch of acidic residues on the open side of the β-sheet. This region forms crystal contacts to partly disordered residues 1–10 of a symmetry-related molecule. Residues 343–352 at the C terminus form a small β-hairpin which contacts S5 and H4 of the GTPase domain. Residues 357–372 are disordered in the crystal. The electron density for the C-terminal domain is slightly weaker than for the GTPase domain, probably because the C-terminal domain has only a few crystal contacts.

As predicted[16,17], GDP binding to FtsZ is different from typical GTPases[18], although the GTPase domain of FtsZ is related to the fold of typical GTPases like p21^{ras}. Six distinct sequence regions in FtsZ make contacts to the nucleotide: loops T1–T4 (tubulin loops) and two regions for sugar binding and guanine binding, respectively (Fig. 2). The GTPase domain starts with the typical strand–loop–helix motif between S1 and H1, but the conformation of this loop is different from that in classical P-loop proteins. FtsZ makes three additional contacts to the nucleotide's phosphates: loop T2 between S2 and HL1, loop T3 between S3 and H2A, and loop T4 between S4 and H3 carrying the tubulin signature motif. All four loops make mainly backbone contacts to the phosphates. As FtsZ was crystallized in the presence of EDTA, we did not expect to find a magnesium ion complexed to GDP. A poorly ordered water molecule (WAT472) occupies a similar position to the magnesium ion in p21^{ras}–GDP[13]; however, WAT482 is complexed between the β-phosphate and Asn 70, which makes it unlikely that this position in FtsZ would be occupied by a positively charged magnesium ion. Furthermore, it has been reported that nucleotide binding to FtsZ, but not nucleotide hydrolysis, is independent of magnesium[19]. The structure displays a pocket for the γ-phosphate and we found that fresh crystals showed weak electron density for a γ-phosphate. We think it is possible that GTP, originally bound to the protein, is slowly hydrolysed in the crystals. We were not able to detect large conformational changes between new and old crystals but the molecule may be fixed in one state by crystal restraints. The loop between S5 and H4 contains two residues that specifically bind the sugar moiety of the nucleotide (Fig. 3): Glu 165 hydrogen-bonds with the two hydroxyl groups O2′ and O3′ and Arg 169 makes contacts to the O5′ hydroxyl and the α-phosphate. Guanine recognition is mainly accomplished by residues within H5: Asp 212 points to N1 and Phe 208 stacks on the aromatic ring. This aromatic stack is extended by Phe 162 and Phe 196. Leu 215 makes a hydrophobic contact on the other side of the guanine.

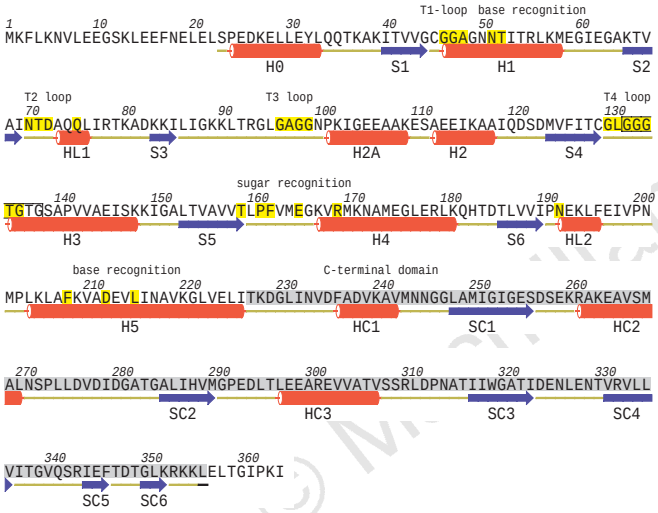

Figure 2 Secondary structure assignment of FtsZ1 from *M. jannaschii*. The secondary structure of FtsZ determined from the crystal structure was calculated with DSSP[29]. The numbering of secondary structure elements follows the p21^{ras} nomenclature[13]. Elements in the C-terminal domain are numbered SC and HC for strands and helices, respectively. Residues highlighted in yellow make contact with GDP. Residues of the C-terminal domain are shaded. Prepared using ALSCRIPT[30].

Table 1 Crystallographic data

Space group $I2_13$ (199)	NATI2	NATI1	Thiomersal (3 mM) EMTS1 (48 h)	Thiomersal (3 mM) EMTS3 (18 h)
Temperature	100 K	RT	RT	RT
Resolution (Å)	2.8	3.7	4.0	4.2
Completeness (%)	99.0 (99.7)	97.3	90.2	97.1
R_{merge}*	0.065 (0.31)	0.12	0.14	0.15
$I/\sigma(I)$ last shell	2.3	1.7	1.6	2.1
R_{iso}†			0.19	0.16
Phasing power‡			1.88	1.83
Refinement				
Model	Residues 23–356, 1 GDP and 116 water molecules			
Data	NAT12, 8–2.8 Å, all reflections			
R factor	0.199 (R_{free} 0.282§)			
R.m.s. deviations	Bonds: 0.012 Å, angles: 1.77°; temperature factors: 3.4 Å^2			

Completeness and R_{merge} for the outermost shell (2.80–2.95 Å) are in parentheses for NATI2.
*R_{merge}: $\Sigma_h \Sigma_i |I(h,i) - \langle I(h)\rangle| / \Sigma_h \Sigma_i I(h,i)$ where $I(h,i)$ are symmetry-related intensities and $\langle I(h)\rangle$ is the mean intensity of the reflection with unique index h.
†R_{iso}: $2\Sigma_h |F_{PH} - F_P| / \Sigma_h |F_P + F_{PH}|$ where F_{PH} and F_P are the derivative and native structure factor amplitudes, respectively.
‡ Phasing power: mean value of the heavy-atom structure amplitudes divided by the residual lack-of-closure. Figure of merit was 0.59 and 0.42 for centric and acentric reflections, respectively.
§ Five per cent of reflections were selected for determination of free *R* factor.

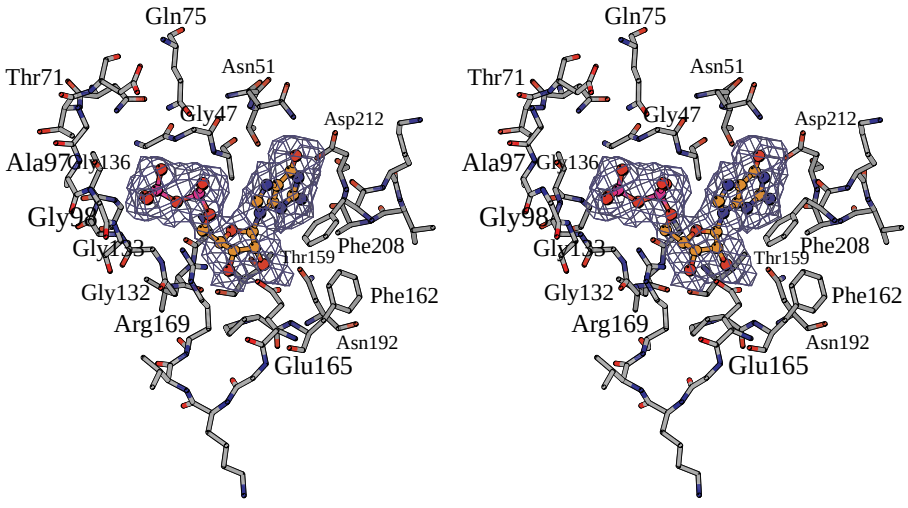

Figure 3 Stereo plot of the active site of FtsZ. Superimposed is the final $2F_0$–F_c electron density map for the nucleotide contoured at 1σ. Prepared with MOLSCRIPT[28].

Asn 51 forms a hydrogen bond with O6 of the base. By contacting H5, the nucleotide may induce a conformational change during hydrolysis, moving the relative orientation of the catalytic domain and the C-terminal domain. A region around Gly 221 may deliver the flexibility between the two β-sheets for this type of movement. As in other GTPases, no residue could be identified that provides an activated nucleophile for hydrolysis. A comparison between the active sites of FtsZ and $p21^{ras}$ in the GDP-bound state[13] reveals important differences: the P-loop in $p21^{ras}$ (G1 box, residues 10–17) has no counterpart in FtsZ but is probably functionally related to loops T1 and T4 in FtsZ. Residues in T1 and T4 make backbone contacts to the phosphates (residues 44–48 and 130–136, containing the tubulin signature motif). Thr 135 of FtsZ is approximately in the same position as Ser 17 of $p21^{ras}$. The T2 loop in FtsZ (residues 70–75) is approximately in the same place as the residues of the G2 box of $p21^{ras}$ (residues 32–37). Asp 72 of FtsZ is the only acidic side chain in the active site of FtsZ and may be the equivalent of Asp 57 of $p21^{ras}$. Loop T3 in FtsZ (residues 94–99) is nearly in the same place as G box G3 of $p21^{ras}$ (residues 57–60) with respect to the phosphates. Residues Lys 117 and Asp 119, located in a loop between S5 and S6, make the most important contacts to the guanine ring in $p21^{ras}$. The equivalent residues in FtsZ are Phe 208 and Asp 212, respectively. These residues are located in helix H5 in FtsZ. The sugar moiety in FtsZ is rotated by ~180° with respect to $p21^{ras}$ if the central β-sheet of the two proteins is aligned. The residue making the hydrogen bonds to O2′ and O3′ in $p21^{ras}$ is located in the first half of the sequence ($p21^{ras}$ Asp 30), whereas the corresponding residue in FtsZ (Glu 165) is located in the second half of the GTPase domain in the sugar-binding loop (residues 159–169). Sequence comparisons between tubulins and FtsZ had already revealed limited homology of ~10–18% identity[7,19,20]. Sequence alignment based on the structure of FtsZ alone (data not shown) revealed that most residues involved in GDP binding and several structural glycines and prolines are conserved and made it likely that the GTPase domain of tubulin is a Rossmann fold as well. The C-terminal domain of tubulins is larger and has very limited sequence homology to FtsZ, possibly reflecting diverse differences between the variety of interacting molecules. Strong structural similarity between FtsZ and tubulin both in the GTPase and the C-terminal domain is now evident from comparing the structure of FtsZ with the two-dimensional crystal structure of α- and β-tubulin[10]. Tubulin lacks the N-terminal extension of FtsZ but contains a large insertion between H1 and S2. Two large helices in tubulin extend the C-terminal domain. Nucleotide binding is very similar between FtsZ and β-tubulin, with many residues involved in GDP binding being conserved.

The 22 partly disordered N-terminal residues stick out of the molecule and make important crystal contacts, as do the last visible residues at the C terminus, which form a twofold contact with symmetry-related residues of another molecule. Inspection of the crystal packing reveals no obvious protofilament structures, as expected for a crystal packing with one molecule per asymmetric unit and a high-symmetry space group. The exposed N terminus with ~33 residues sticking out of the compact GTPase domain is rapidly degraded by proteases in the C41 expression host. Comparison between different FtsZ sequences reveals that this N-terminal extension is highly variable and is very short in *E. coli*, where it starts at residue 28, so it is unlikely to be important in filament formation. The C terminus is visible up to residue 356, with eight residues of the wild-type protein and the additional eight residues of the His_6-tagged protein being disordered. The C termini of FtsZ sequences are divergent from residue 342 onwards, after the last sheet of the C-terminal domain. Both the C and N termini contain many acidic residues and acidic/hydrophobic repeats. These sequences could simply enhance the solubility of monomers or filaments, although other functions have been proposed for the C termini of tubulins[21]. FtsZ(MJ0370) from *M. jannaschii* contains two cysteines, Cys 129 and Cys 45, which lie near the active-site strands S1 and S4 in the GTPase domain: this geometry would allow formation of a disulphide bridge and one mercury atom can bind to both residues. Because of its high similarity to tubulin, FtsZ should prove to be a simple model system for microtubule dynamics and be amenable to protein engineering. □

Methods

Protein expression, purification and crystallization. Genomic DNA was extracted from a living culture of *M. jannaschii* (DSM 2661, ATCC 43067) with a commercial kit (Promega Wizard). Genomic PCR using two primers (5′-GAACTGCCATATGAAATTTCTAAAAAACGTTTTA-3′, 5′-CGTATTAGGATCCAATTTTTGGAATTCCTGTGTGTTCTA-3′), replacing the GTG start codon with ATG, produced a 1,115-bp DNA carrying the complete 1,092 bp of MJ0370 and unique cleaving sites for *Nde*I and *Bam*HI. This fragment was cloned into the pHis17 vector (B. Miroux, personal communication), putting it under control of a T7-promoter and adding eight residues at the C terminus (GSHHHHHH) to yield a protein of 372 residues. C41 cells[12] were transformed and expressed the His-tagged protein after addition of IPTG. After induction in log phase, cells from a 10-litre culture were collected and snap-frozen in liquid nitrogen. The frozen pellet was powdered under liquid nitrogen and poured directly into 200 ml of boiling buffer A (50 mM Tris-HCl, 300 mM NaCl, pH 8.0) and stirred for 90 s. After addition of ice to a final volume of 400 ml, the lysate was centrifuged and applied to a Ni-NTA column (Qiagen). The FtsZ protein eluted at ~400–450 mM imidazole in buffer A, pH 6.0. The protein was further purified on a Sepharose-6B column (Pharmacia) using 20 mM Tris-HCl, 1 mM EDTA, 1 mM NaN_3. FtsZ eluted as an oligomer under low-salt conditions. The product was checked by electrospray mass spectrometry (observed: 39,889.12 g mol^{-1}; estimated: 39,891.33 g mol^{-1}). Crystals were grown by the hanging-drop vapour-diffusion technique using 0.1 M MES pH 6.62, 17% PEG400 and 6% ethanol as crystallization solution. Droplets composed of 3 parts of 10 mg ml^{-1} protein solution and 1 part crystallization solution were equilibrated for a minimum of one week. Two different crystal forms grew under these conditions, distinguishable by the lack of birefringence for one of them. These latter crystals belong to cubic spacegroup $I2_13$, with one molecule per asymmetric unit and 71% solvent content; cell dimensions are $a = b = c = 159.14$ Å, with all angles 90°. Crystals for multiple isomorphous replacement were collected in crystallization solution and mounted in sealed capillaries. A crystal for the frozen dataset NATI2 was collected in crystallization solution and soaked for 5 min in 0.1 M MES pH 6.62, 25% PEG200 and 6% ethanol and frozen in a stream of cold nitrogen at 100 K.

Structure determination and refinement. Each low-resolution dataset was collected from a single crystal, using a MAR imaging-plate detector mounted on an Elliot GX13 rotating anode X-ray generator. The final native dataset NATI2 was collected from a frozen crystal at beamline 9.6 at the Daresbury SRS. Images were indexed and integrated with the MOSFLM[22] package and further processed using the CCP4 suite of programs[23]. The structure was determined by the MIRAS method using only one derivative (ethylmercurithiosalicylic acid, thiomersal, 3 mM) with two different soak times of 18 and 48 h, respectively. Heavy-atom positions were determined using SHELXS[24] and initial phases were calculated with MLPHARE. Phasing statistics are given in Table 1. After 20 cycles of phase refinement using SOLOMON[25] and phase extension from 4.0 to 3.7 Å resolution, a superb electron density map was obtained. Residues 1–356 could be built into the first density using FRODO[26], although the density for residues 1–22 was weak and these residues were later omitted from the final model. Crystallographic refinement was performed using the programs REFMAC (room-temperature data sets; phase-restrained) and X-PLOR[27]. A total of 26 cycles of refinement and manual rebuilding was necessary to switch from the unfrozen to the frozen native dataset. At 2.8 Å resolution, solvent mask correction was applied and a resolution range of 8.0–2.8 Å was used. No reflections were excluded from refinement by their signal-to-noise ratio. The current model contains residues 23–356, 116 water molecules and 1 GDP molecule. Residues 1–22 gave weak difference density but were not refineable. The model shows good geometry with an r.m.s. deviation over bond length of 0.012, bond angles of 1.77° and no Ramachandran outliers. Individual temperature factors have been refined using tight restraints. They are higher for the C-terminal domain (residues 227–356), with an overall temperature

factor over residues 23–356 of 53 Å^2 (65 Å^2 from the Wilson plot). Coordinates and structure factors have been deposited in the Brookhaven Protein Data Bank.

Received 4 August; accepted 20 October 1997.

1. Rothfield, L. I. & Justice, S. S. Bacterial cell division: the cycle of the ring. *Cell* **88,** 581–584 (1997).
2. Donachie, W. D. The cell cycle of *Escherichia coli*. *Annu. Rev. Microbiol.* **47,** 199–230 (1993).
3. Erickson, H. P. FtsZ, a tubulin homologue, in prokaryote cell division. *Trends Cell Biol.* **7,** 362–367 (1997).
4. Lutkenhaus, J. FtsZ ring in bacterial cytokinesis. *Mol. Microbiol.* **9,** 403–409 (1993).
5. de Boer, P., Crossley, R. & Rothfield, L. The essential bacterial cell-division protein FtsZ is a GTPase. *Nature* **359,** 254–256 (1992).
6. RayChaudhuri, D. & Park, J. T. *Escherichia coli* cell-division gene FtsZ encodes a novel GTP-binding protein. *Nature* **359,** 251–254 (1992).
7. Erickson, H. P. FtsZ, a prokaryotic homolog of tubulin? *Cell* **80,** 367–370 (1995).
8. Bramhill, D. & Thompson, C. M. GTP-dependent polymerization of *Escherichia coli* FtsZ protein to form tubules. *Proc. Natl Acad. Sci. USA* **91,** 5813–5817 (1994).
9. Mukherjee, A. & Lutkenhaus, J. Guanine nucleotide-dependent assembly of FtsZ into filaments. *J. Bacteriol.* **176,** 2754–2758 (1994).
10. Nogales, E., Wolf, S. G. & Downing, K. H. Structure of the αβ tubulin dimer by electron crystallography. *Nature* **391,** 199–203 (1998).
11. Bult, C. J. *et al*. Complete genome sequence of the methanogenic archaeon, *Methanococcus jannaschii*. *Science* **269,** 496–512 (1996).
12. Miroux, B. & Walker, J. E. Over-production of proteins in *Escherichia coli*: Mutant hosts that allow synthesis of some membrane proteins and globular proteins at high levels. *J. Mol. Biol.* **260,** 289–298 (1996).
13. Tong, L., de Vos, A. M., Milburn, M. V. & Kim, S.-H. Crystal structures at 2.2 Å resolution of the catalytic domains of normal ras protein and an oncogenic mutant complexed with GDP. *J. Mol. Biol.* **217,** 503–513 (1991).
14. Rossmann, M. G., Moras, D. & Olsen, K. Chemical and biological evolution of a nucleotide-binding protein. *Nature* **250,** 194–199 (1974).
15. Chook, Y. M., Gray, J. V., Ke, H. & Lipscomb, W. N. The monofunctional chorismate mutase from *Bacillus subtilis*: structure determination of chorismate mutase and its complexes with a transition state analog and prephenate, and implications on the mechanism of enzymatic reaction. *J. Mol. Biol.* **240,** 476–500 (1994).
16. Linse, K. & Mandelkow, E.-M. The GTP-binding peptide of β-tubulin. *J. Biol. Chem.* **263,** 15205–15210 (1988).
17. Sage, C. R. *et al*. Site-directed mutagenesis of putative GTP-binding sites of yeast β-tubulin: evidence that α-, β- and γ-tubulins are atypical GTPases. *Biochemistry* **34,** 16870–16875 (1995).
18. Bourne, H. R., Sanders, D. A. & McCormick, F. The GTPase superfamily: conserved structure and molecular mechanism. *Nature* **349,** 117–127 (1991).
19. Mukherjee, A., Dai, K. & Lutkenhaus, J. *Escherichia coli* cell division protein FtsZ is a guanine nucleotide binding protein. *Proc. Natl Acad. Sci. USA* **90,** 1053–1057 (1993).
20. de Pereda, J. M., Leynadier, D., Evangelio, J. A., Chacon, P. & Andreu, J. M. Tubulin secondary structure analysis, limited proteolysis sites, and homology to FtsZ. *Biochemistry* **35,** 14203–14215 (1996).
21. Sackett, D. L. Structure and function in the tubulin dimer and the role of the acidic carboxyl terminus. *Subcell. Biochem.* **24,** 255–302 (1995).
22. Leslie, A. G. W. *Recent changes to the MOSFLM package for processing film and image plate data* (SERC Laboratory, Daresbury, Warrington, UK, 1991).
23. The CCP4 suite: Programs for protein crystallography. *Acta Crystallogr. D* **54,** 760–763 (1994).
24. Sheldrick, G. M. Heavy atom location using SHELXS-90. In *Isomorphous Replacement and Anomalous Scattering: Proceedings of the CCP4 Study Weekend 25–26 January 1991* (eds Wolf, W., Evans, P. R. & Leslie, A. G. W.) 23–38 (SERC Daresbury Laboratory, Warrington, UK, 1991).
25. Abrahams, J. P. & Leslie, A. G. W. Methods used in the structure determination of bovine mitochondrial F1-ATPase. *Acta Crystallogr. D* **52,** 30–42 (1996).
26. Jones, T. A. A graphics model building and refinement system for macromolecules. *J. Appl. Cryst.* **11,** 268–272 (1978).
27. Brünger, A. *X-PLOR Version 3.1, A System for X-ray Crystallography and NMR* (Yale University Press, New Haven and London, 1992).
28. Kraulis, P. J. MOLSCRIPT: a program to produce both detailed and schematic plots of protein structures. *J. Appl. Cryst.* **24,** 946–950 (1991).
29. Kabsch, W. & Sander, C. Dictionary of protein secondary structure: pattern recognition of hydrogen bonded and geometrical features. *Biopolymers* **22,** 2577–2637 (1983).
30. Barton, G. J. ALSCRIPT: a tool to format multiple sequence alignments. *Prot. Eng.* **6,** 37–40 (1993).

Acknowledgements. We thank H. Huber (University of Regensburg) for *M. jannaschii* cells, I. Fearnley for mass spectrometry, B. Miroux for C41 cells and for discussion, and A. Murzin for pointing out the similarity to chorismate mutase. J.L. is supported by an EMBO long-term fellowship.

Correspondence and requests for materials should be addressed to J.L. The identity codes for the FtsZ coordinates and structure factors in the Protein Data Bank are 1FSZ and R1FSZSF, respectively.